ENGINEERING MECHANICS 2009
National Conference with International Participation
Svratka, Czech Republic, May 11 – 14, 2009

pp. 1065–1078
Paper **#239**

TRAVELLING WAVES IN ROTATIONAL MACHINES

L. Půst, L. Pešek [1]

Summary: *This paper is concerned with vibrations of stationary or rotating disk as a simplified model of real bladed turbine disk. Two types of disks are investigated: perfect rotational disk with the same dynamic properties in all radial directions and imperfect disk having different dynamic properties in two independent modes of vibration. Presented study is first part of theoretical analysis intended as a background for evaluation method used in experimental research of vibrations of bladed disk in real rotational machines or their models.*

1. Introduction

Travelling wave is one of the many various forms of vibrations of mechanical systems. It is typical of rotation form of vibration, which can be produced not only by rotating excitation, but in some special causes by fixed standing excitation.

Travelling waves were recorded mainly in circular machine elements as turbine disks, saw blades, computer floppy and hard disks, geared disks, cylindrical shells, circular rings and diaphragms [1-7], but can exists also in non-circular elements as square-shaped plates and membranes having pairs of equal or very near lying eigenfrequencies with similar modes [4]. However the most important and also dangerous cases of travelling waves in mechanical engineering are connected with vibrations of rotating disks of steam or gas turbines. Lot of articles were published in recent years e.g. [5,6,8-10] both for simple disks and for bladed disks.

Presented paper is a contribution to the problems of travelling waves of bladed disk aimed particularly as a theoretical background for analysis of results of measurement on the experimental model in laboratories IT-AS CR.

Sixty prismatic models of blades were fastened on the perimeter of investigated model of steel disk with diameter 505 mm. The disk is fixed in the centre 0. Two groups of five blades lying on opposite ends of a diameter identical with axis *y* are provided by heads with dry friction elements, Fig. 1.

Due to this imperfection in distribution of mass, the free oscillations with the same number of nodal diameters and nodal circles, once with a node line going through this imperfection and other time with maximum amplitude (antinode), have different frequencies.

Frequence-difference is roughly proportional to the imperfection. For exact rotation form of disk without any added mass, the disk has double frequencies, each with two different

[1] Ing. Ladislav Půst, DrSc, Ing. Luděk Pešek,CSc, Institute of Thermomechanics AS CR, v.v.i., Dolejškova 5, 18200 Praha 8, e-mail: pust@it.cas.cz, , pesek@it.cas.cz

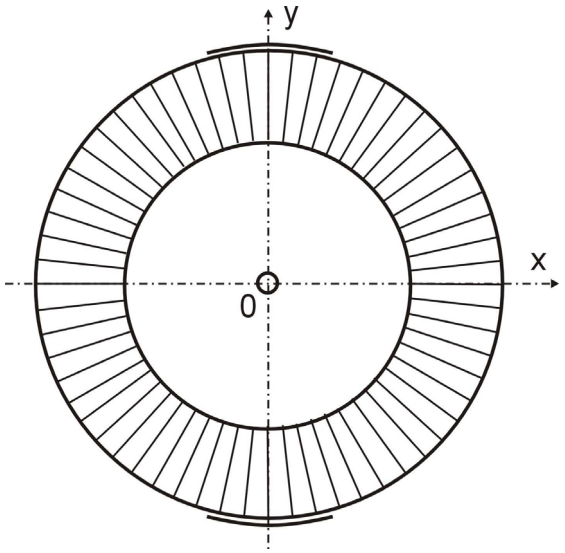

Fig. 1

modes of oscillation. An example of oscillations modes of free circular ring is shown in Fig. 2. In the three columns are modes of three eigenfrequencies Ω_1, Ω_2, Ω_3 of cylindrical ring. To each of these frequencies belong two orthogonal eigenmodes with modal points shifted at $\varphi = \pi / 2n$ (n = 1,2.3). If a small mass is added in point A, the eigenfrequencies of the upper row a) would be smaller than those of bottom row b). Existence of these pairs of eigenmodes enables to excite travelling waves. Similar dynamic properties has also the circular disk and bladed disk.

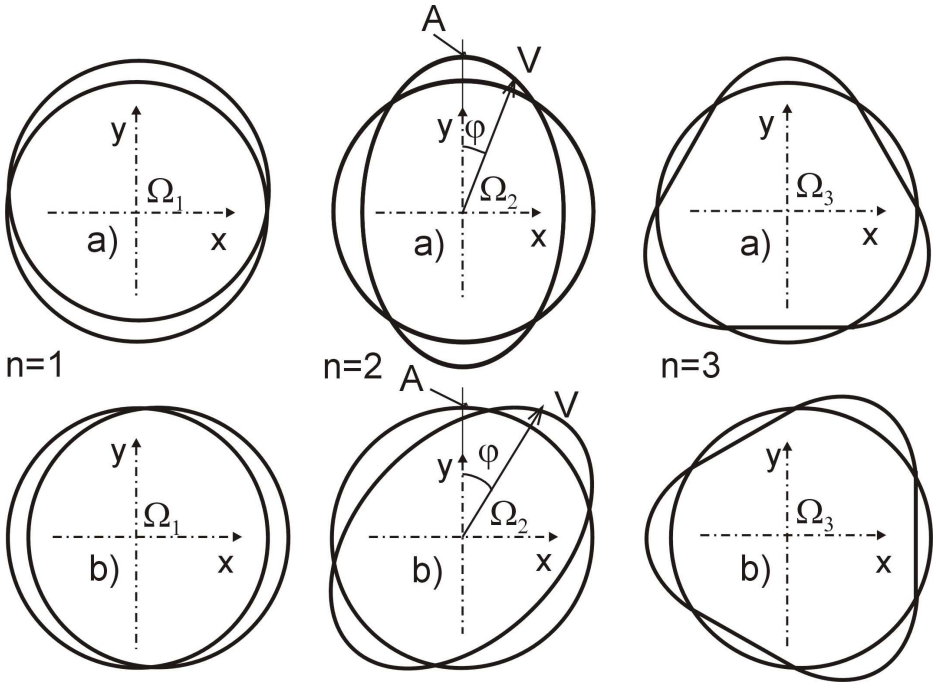

Fig. 2

2. Travelling waves – stationary disk

Free transverse vibrations of circular perfect disks fixed at their centers have modes containing *n* nodal diameters and *l* nodal circles as shown in Fig. 3.

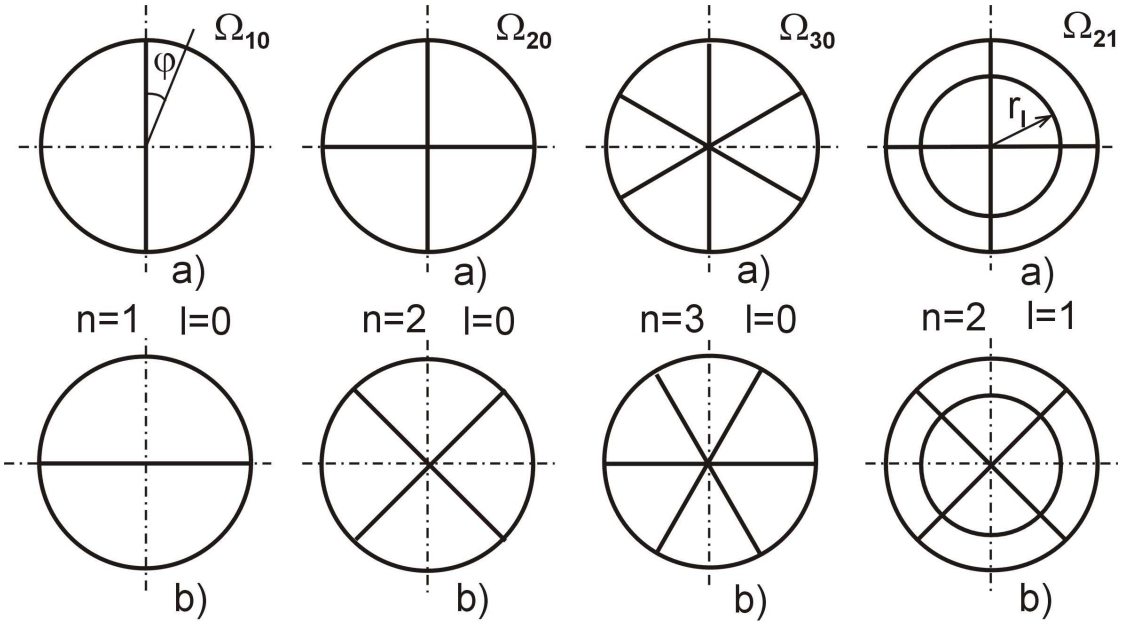

Fig. 3

The forms of vibrations with amplitude a are described by

$$z(r,\varphi) = a f_l(r)\sin n(\varphi+\alpha)\,, \tag{1}$$

where $r=\sqrt{x^2+y^2}$, $f_l(r)$ denotes the form of vibration in the radial direction. Roots r_l of equation

$$f_l(r) = 0 \tag{2}$$

give the radii of nodal circles. Values of parameter α ascertain the position of nodal diameters. Value $\alpha = 0$ corresponds to the nodal diameters in upper row a) in Fig. 3, value $\alpha = \pi/(2n)$ to the position of nodal lines in bottom row b). Proper initial conditions in time $t = 0$ produce the combination of both eigenmodes with common eigenfrequency Ω_{nl} of the undamped disk:

$$z(r,\varphi,t) = a_a f_l(r)\sin n\varphi\cos(\Omega_{nl}t+\varphi_a) + a_b f_l(r)\cos n\varphi\cos(\Omega_{nl}t+\varphi_b) \tag{3}$$

This motion contains both eigen oscillations of a) and b) forms and also a component of travelling wave, which is composed of parts of forms a) and b) with the same amplitudes

$$\begin{aligned} z_t(r,\varphi,t) &= a_t f(r)\sin n\varphi\cos(\Omega_{nl}t+\varphi_t) + a_t f(r)\cos n\varphi\sin(\Omega_{nl}t+\varphi_t) = \\ &= a_t f(r)\sin(n\varphi+\Omega_{nl}t+\varphi_t). \end{aligned} \tag{4}$$

Traveling wave in undamped disk have the form

$$z_t(r,\varphi) = a_t f(r)\sin n(\varphi+\varphi_t/n)\,, \tag{5}$$

which rotate on the disk by angular frequency

$$\frac{d\varphi}{dt} = \frac{\Omega_{nl}}{n} \quad \text{or} \quad \frac{d\varphi}{dt} = -\frac{\Omega_{nl}}{n} \tag{6}$$

according to the values of initial conditions. However a damping in real disk makes a quick decay of these free travelling wave oscillations.

Only travelling external force can excite travelling waves in perfect damped circular disk. The nodal diameters travel then according to the force rotation. Stationary harmonic force excites non-travelling oscillations in perfect disk.

Another situation originates when the disk has small imperfection, caused e.g. by added mass on the periphery. This is the case of bladed disk shown in Fig. 1. Simplified scheme of disk fixed in center and with nodal diameters of n = 2, l = 0 is in Fig. 4.

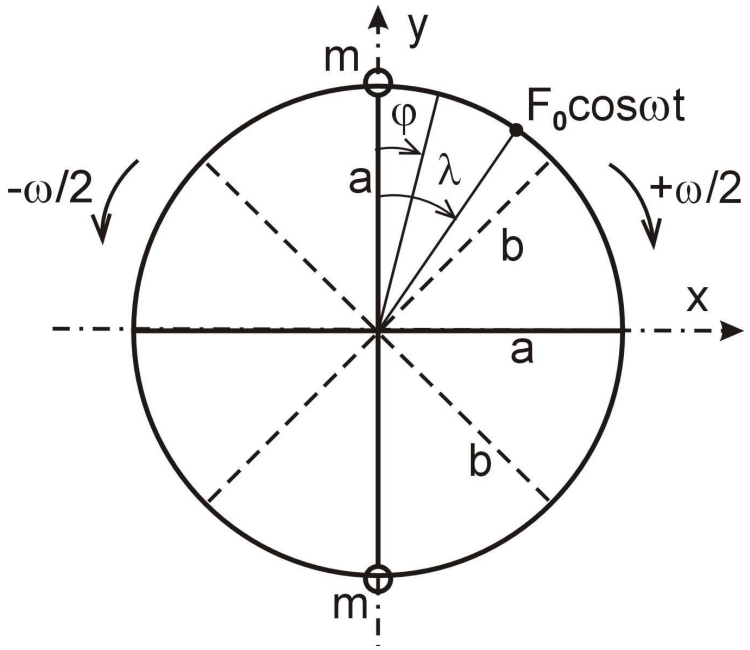

Fig. 4

Positions of nodal diameters are now determined by positions of small added masses m. There is no double frequency Ω_{20} as in Fig. 3 for perfect disk but due to the imperfection this frequency splits into two close frequencies Ω_{2a} and Ω_{2b} belonging to two modes of vibration with different modal diameters: the higher Ω_{2a} with masses m on the nodal diameters and the lower Ω_{2b} where the masses m vibrate in antinode position – nodal lines are dashed.

If general initial conditions are applied to this imperfect disk the resulting vibrations are very complicated. Internal or/and external damping attenuates these free oscillations to zero and no stationary travelling wave exists.

Let us apply an external harmonic transverse force $F_0 \cos \omega t$ in one point given by angle λ on the periphery of the linearly damped imperfect disk. If the exciting frequency ω is close to eigenfrequencies Ω_{2a} and Ω_{2b}, corresponding components predominate over other non-resonant components and the response can be described only by these two modes of vibrations.

The amplitudes z_a, z_b of these components can be expressed by means of the procedure described in [1,5] in the forms

$$z_a = \frac{K_a f(r) \sin 2\varphi \, F_0 \sin 2\lambda}{\sqrt{(\Omega_a^2 - \omega^2)^2 + b_1^2 \omega^2}} \cos(\omega t - \psi_a),$$
$$z_b = \frac{K_b f(r) \cos 2\varphi \, F_0 \cos 2\lambda}{\sqrt{(\Omega_b^2 - \omega^2)^2 + b_2^2 \omega^2}} \cos(\omega t - \psi_b), \tag{7}$$

where $K_a f(r)$ and $K_b f(r)$ are functions depending on the structure and mass distribution of bladed disk, λ is angle ascertaining point of exciting force application, Ω_a and Ω_b are split eigenfrequencies, b_a, b_b damping coefficients and phase angles for each mode are

$$\psi_a = \tan^{-1}\frac{b_a\omega}{\Omega_a^2-\omega^2}, \quad \psi_b = \tan^{-1}\frac{b_b\omega}{\Omega_b^2-\omega^2}. \tag{8}$$

For simplicity we can assume that $K_a = K_b = K, \quad b_a = b_b = b.$

Dimensionless forms of equations (7), (8) are

$$\begin{aligned} Z_a &= \frac{\sin 2\varphi \sin 2\lambda}{\sqrt{(1-\eta^2)^2+\beta^2\eta^2}}\cos(\omega t-\psi_a), \\ Z_b &= \frac{\cos 2\varphi \cos 2\lambda}{\sqrt{(\kappa^2-\eta^2)^2+\beta^2\eta^2}}\cos(\omega t-\psi_b), \\ \psi_a &= \tan^{-1}\frac{\beta\eta}{1-\eta^2}, \quad \psi_b = \tan^{-1}\frac{\beta\eta}{\kappa^2-\eta^2}, \end{aligned} \tag{9}$$

where

$Z_i = \dfrac{z_i\Omega_a^2}{Kf(r)F_0}$ are dimensionless local amplitudes (i = a,b),

$\kappa = \dfrac{\Omega_b}{\Omega_a}$ is ratio of split eigenfrequencies and $\beta = \dfrac{b}{\Omega_a}$, $\eta = \omega/\Omega_a$. (9a)

If the force $F_0\cos\omega t$ acts on the end of diameter a) (λ = 0), the eigenmode with lower frequency Ω_b with nodes *b* is excited. If the force acts on nodal diameter b) i.e. if $\lambda = \pi/4$, eigenmode with higher frequency Ω_a with nodes *a* originate. Response for forces in positions $\lambda = \pi/16$, $\pi/8$ and $\pi 3/16$ and for $\kappa = 0.97$, $\beta = 0.02$ are shown in Fig. 5, where both components of vibrations are excited and their amplitudes are

$$\begin{aligned} A_a &= \max Z_a = \frac{\sin 2\lambda}{\sqrt{(1-\eta^2)^2+\beta^2\eta^2}}, \\ A_b &= \max Z_b = \frac{\cos 2\lambda}{\sqrt{(\kappa^2-\eta^2)^2+\beta\eta^2}}. \end{aligned} \tag{10}$$

Corresponding phase shift angles ψ_a and ψ_b are independent on the position of exciting force defined by angle λ, as seen from the bottom row of subfigures in Fig. 5.

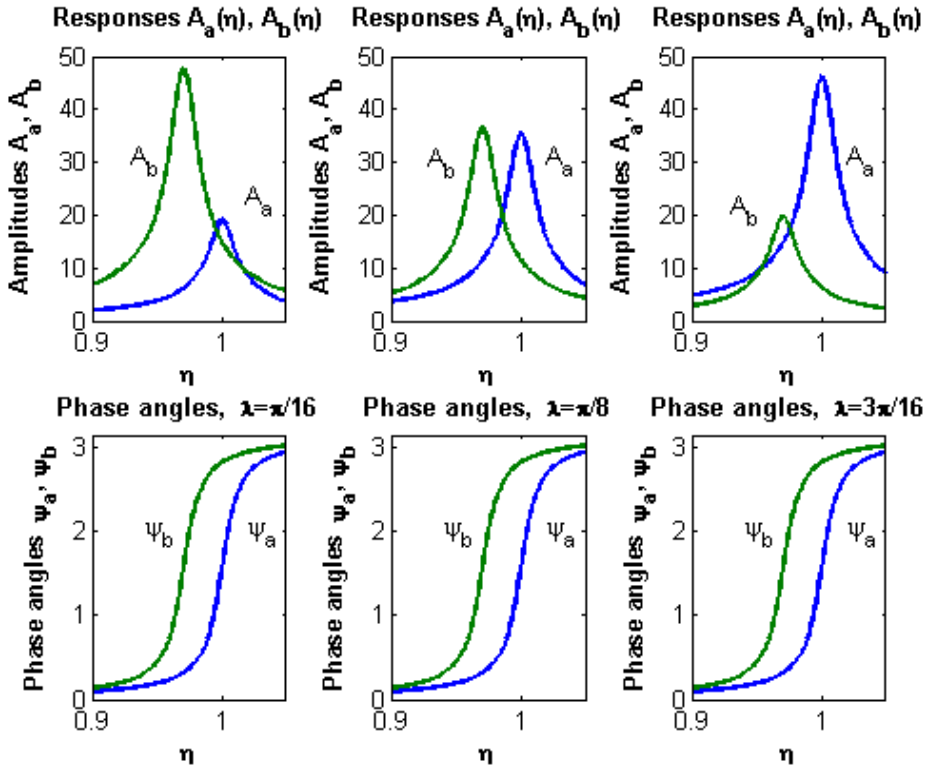

Fig. 5

In the next Fig. 6 are shown only response curves for the same values of $\kappa = 0.97$, $\beta = 0.02$ and for the extended range $\lambda = 0 - \pi/4$ but without phase shift angles. The increase of amplitude A_a of mode *a* versus dimensionless frequency η and decrease of A_b (mode *b*, frequency $\eta_b = \kappa = \Omega_a/\Omega_b$) is quite evident.

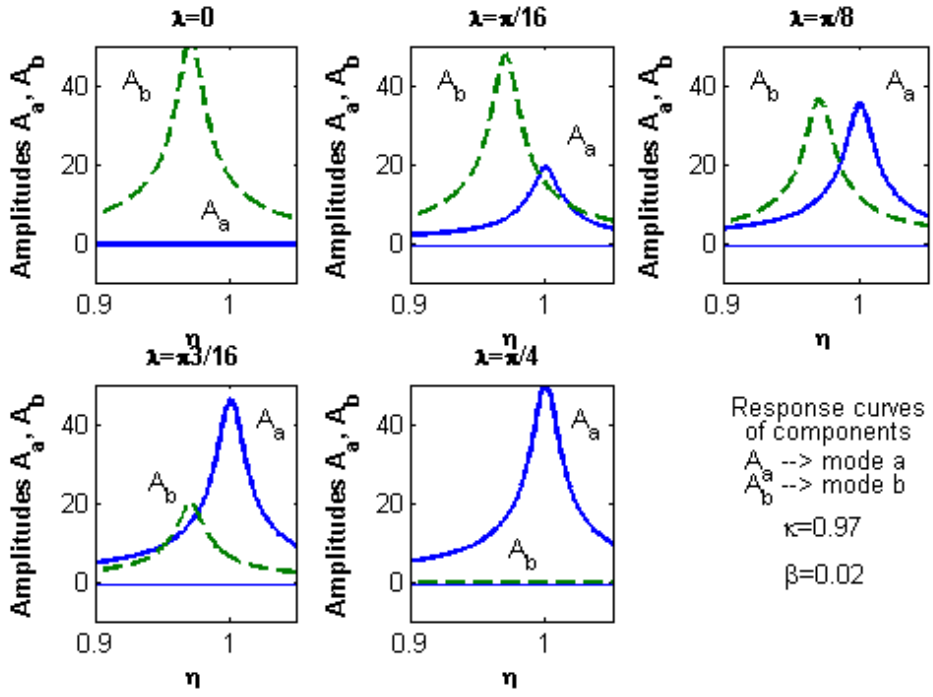

Fig. 6

The complete response of disk on exciting force consists of sum of both components:

$$Z = Z_a + Z_b = A_a \sin 2\varphi \cos(\omega t - \psi_a) + A_b \cos 2\varphi \cos(\omega t - \psi_b) = \tag{11}$$
$$= A_a \sin 2\varphi(\cos\omega t \cos\psi_a + \sin\omega t \sin\psi_a) + A_b \cos 2\varphi(\cos\omega t \cos\psi_b + \sin\omega t \sin\psi_b) =$$
$$= A_a \cos\psi_a \frac{\sin(2\varphi - \omega t) + \sin(2\varphi + \omega t)}{2} + A_a \sin\psi_a \frac{-\cos(2\varphi + \omega t) + \cos(2\varphi - \omega t)}{2} +$$
$$+ A_b \cos\psi_b \frac{\cos(2\varphi + \omega t) + \cos(2\varphi - \omega t)}{2} + A_b \sin\psi_b \frac{-\sin(2\varphi - \omega t) + \sin(2\varphi + \omega t)}{2}.$$

where the arguments $(2\varphi \pm \omega t)$ signify the existence of travelling waves.

After rearrangement (11) we get

$$\begin{aligned} Z &= (A_a \cos\psi_a + A_b \sin\psi_b)/2 * \sin(2\varphi + \omega t) + \\ &+ (-A_a \sin\psi_a + A_b \cos\psi_b)/2 * \cos(2\varphi + \omega t) + \\ &+ (A_a \cos\psi_a - A_b \sin\psi_b)/2 * \sin(2\varphi - \omega t) + \\ &+ (A_a \sin\psi_a + A_b \cos\psi_b)/2 * \cos(2\varphi - \omega t) = \\ &= \sqrt{A_a^2 - 2A_a A_b \sin(\psi_a - \psi_b) + A_b^2}\ /2 * \cos(2\varphi + \omega t + \varepsilon_-) + \\ &+ \sqrt{A_a^2 + 2A_a A_b \sin(\psi_a - \psi_b) + A_b^2}\ /2 * \cos(2\varphi - \omega t + \varepsilon_+) = \\ &= A_{r-} \cos(2\varphi + \omega t + \varepsilon_-) + A_{r+} \cos(2\varphi - \omega t + \varepsilon_+). \end{aligned} \tag{12}$$

Amplitudes A_{r-} resp. A_{r+} belong to the partial travelling waves with angular velocities

$$\frac{d\varphi}{dt} = -\frac{\omega}{2} \quad \text{resp.} \quad \frac{d\varphi}{dt} = +\frac{\omega}{2}. \tag{13}$$

Positive and negative velocities $\pm\omega/2$ are marked by arrows in Fig. 4. Response curves of amplitudes $A_{r+}(\eta)$ resp. $A_{r-}(\eta)$ are plotted in Fig. 7 by solid resp. dashed lines.

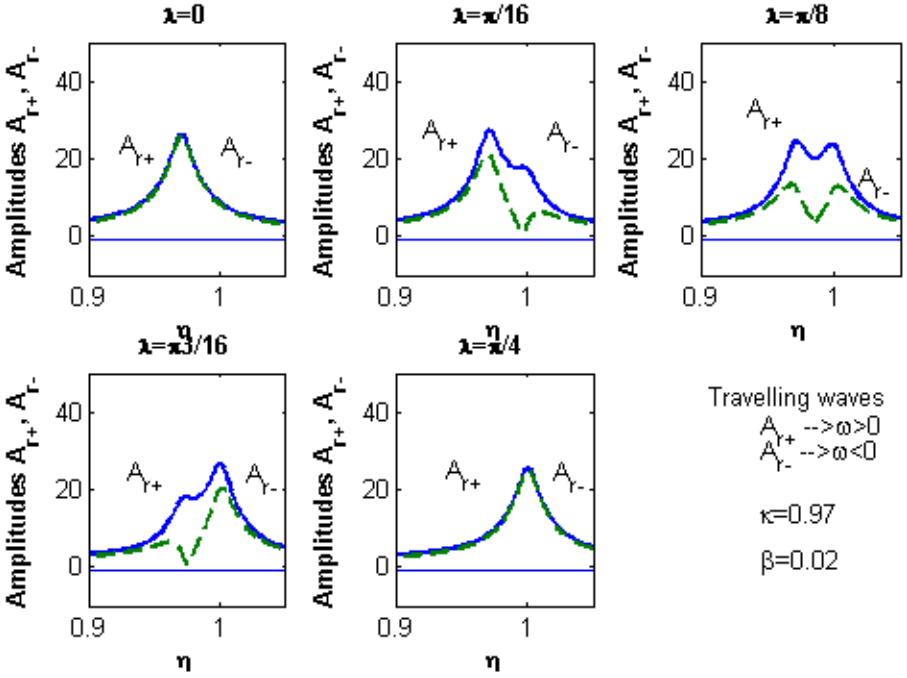

Fig. 7

Sum or difference of these curves (however considering phase angles ε_- and ε_+) gives either stationary vibrations ($\lambda = 0$, $\lambda = \pi/4$) or combination of stacionary vibrations and travelling wave ($0 < \lambda < \pi/4$).

That kind of motion excited by harmonic force in angle position λ is described in the form

$$Z = A_{stac}\cos(2\varphi - 2\lambda)\cos(\omega t - \psi_0) + A_{trav}\cos(2\varphi - 2\lambda - \omega t + \psi_t)\,, \tag{14}$$

where parameters of stationary vibrations A_{stac}, ψ_s and of travelling wave A_{trav}, ψ_t are not yet known. From comparison with the second row of equation (11) we get after small adaptation

$$\begin{aligned} &A_{stac}\left[(\cos 2\varphi\cos 2\lambda) + \sin 2\varphi\sin 2\lambda)(\cos\omega t\cos\psi_s + \sin\omega t\sin\psi_s)\right] + \\ &+ A_{trav}\left[(\cos 2\varphi\cos\omega t + \sin 2\varphi\sin\omega t)\cos(2\lambda - \psi_t)\right] + \\ &+ A_{trav}\left[(\sin 2\varphi\cos\omega t - \cos 2\varphi\sin\omega t)\sin(2\lambda - \psi_t)\right] = \\ &= A_a\sin 2\varphi(\cos\omega t\cos\psi_a + \sin\omega t\sin\psi_a) + A_b\cos 2\varphi(\cos\omega t\cos\psi_b + \sin\omega t\sin\psi_b)\,. \end{aligned} \tag{15}$$

Further comparisons multiplied by $\cos 2\varphi\cos\omega t$, $\cos 2\varphi\sin\omega t$, $\sin 2\varphi\cos\omega t$, $\sin 2\varphi\sin\omega t$ give four equations:

$$\begin{aligned} A_{stac}\cos\psi_s\cos 2\lambda + A_{trav}\cos\psi_t\cos 2\lambda + A_{trav}\sin\psi_t\sin 2\lambda &= A_b\cos\psi_b \\ A_{stac}\sin\psi_s\cos 2\lambda - A_{trav}\cos\psi_t\sin 2\lambda + A_{trav}\sin\psi_t\cos 2\lambda &= A_b\sin\psi_b \\ A_{stac}\cos\psi_s\sin 2\lambda + A_{trav}\cos\psi_t\sin 2\lambda - A_{trav}\sin\psi_t\cos 2\lambda &= A_a\cos\psi_a \\ A_{stac}\sin\psi_s\sin 2\lambda + A_{trav}\cos\psi_t\cos 2\lambda + A_{trav}\sin\psi_t\sin 2\lambda &= A_a\sin\psi_a\,, \end{aligned} \tag{16}$$

from which the four unknown quantities $A_{stac}\cos\psi_s$, $A_{stac}\sin\psi_s$, $A_{trav}\cos\psi_t$, $A_{trav}\sin\psi_t$, resp. $A_{stac}, A_{trav,}\ \psi_s, \psi_t$ can be calculated.

Results of these operations are seen in Fig. 8, where by solid lines are plotted response curves of stationary vibrations $A_{\text{stac}}(\eta)$ and by dashed lines those of travelling waves $A_{\text{trav}}(\eta)$.

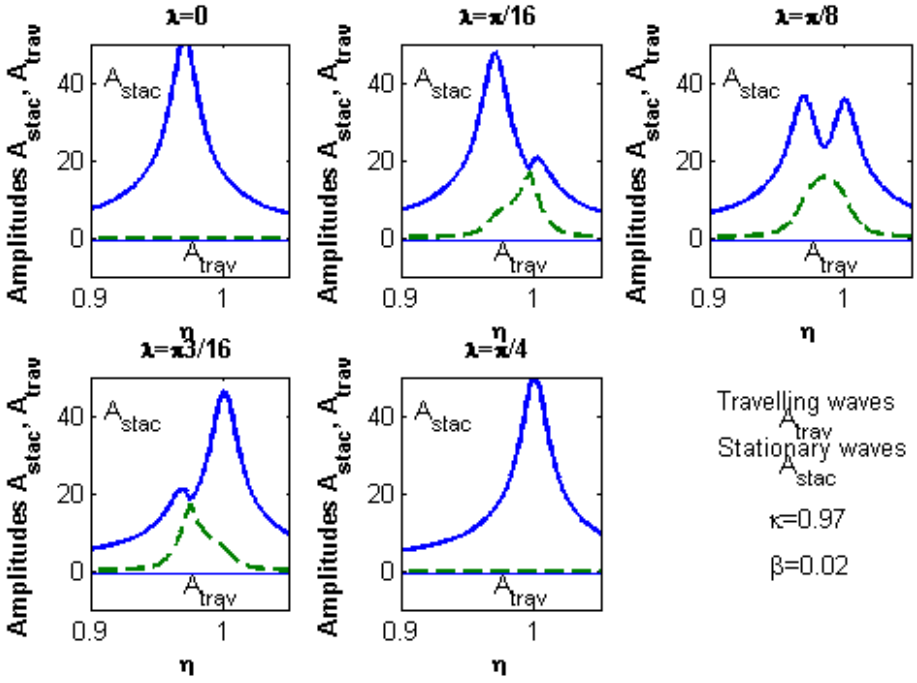

Fig. 8

Similar results we get by applying this procedure also for other mode of vibrations Fig. 3 for nodal diameters n = 1,3,4,… and nodal circles l = 0,1,2…..

3. Rotating disk

Dynamical properties of rotating both perfect an imperfect disk with constant angular speed ν are similar to those of stationary disk. The modes of vibrations have *n* nodal diameters and *l* nodal circles (Fig. 3) but the eigenfrequencies increase with increasing angular velocity ν: $\Omega_{n,l} = \Omega_{n,l,0} + c\nu^2$. This change of frequency is neglected for simplicity in the following analysis. However the response on the excitation force differs from the stationary case.

Two coordinate systems have to be used: 1) a fixed one *r*, φ_a connected with the standing space, and 2) other coordinates connected to the rotating disk. Relation $\varphi = \varphi_a + \nu t$ is valid for initial situation $\varphi = \varphi_a$ at $t = 0$.

Let a harmonic force $F_0 \cos \omega t$ at $\varphi_a = 0$ in the fixed coordinate system acts on rotating perfect disk with angular velocity ν, $\omega \approx \Omega_{20}$ in the negative direction φ. This force excites in the disk (coordinates 2) both modes of vibrations a) and b) (see Fig. 3). Position of force marked $\lambda = -\nu t$ increases in disk coordinates linearly with time.

Vibration of rotating perfect disk (κ = 1) with two nodal diameters (*n* = 2, *l* = 0) can be described using modified formula (9), (9a) by equations

$$\begin{aligned} m_{red}\ddot{q}_a + b_{red}\dot{q}_a + c_{red}q_a &= Kf(r)F_0 \cos\omega t \sin 2\varphi \sin(2\nu t) \\ m_{red}\ddot{q}_b + b_{red}\dot{q}_b + c_{red}q_b &= Kf(r)F_0 \cos\omega t \cos 2\varphi \cos(2\nu t)\,, \end{aligned} \tag{17}$$

where $m_{red}, b_{red}, c_{red}$ are reduced values masses, damping and stiffness.

$$\text{Introducing} \quad u_{a,b} = \frac{q_{a,b} m_{red}}{Kf(r)F_0}\,, \quad \Omega_{20}^2 = \frac{c_{red}}{m_{red}}\,, \quad \beta = \frac{b_{red}}{m_{red}} \tag{18}$$

gives

$$\begin{aligned} \ddot{u}_a + \beta\dot{u}_a + \Omega_{20}^2 u_a &= \cos\omega t \sin 2\varphi \sin 2\nu t \\ \ddot{u}_b + \beta\dot{u}_b + \Omega_{20}^2 u_b &= \cos\omega t \cos 2\varphi \cos 2\nu t\,. \end{aligned} \tag{19}$$

The functions on the right sides of equations (19) are complicated functions of time – product of two harmonic functions. For simple solution of stationary forced vibrations it is convenient to transform these expressions into sum of terms containing just only one harmonic function of time:

$$\begin{aligned} \cos\omega t \sin 2\varphi \sin 2\nu t &= \sin 2\varphi \left[\sin(\omega + 2\nu)t - \sin(\omega - 2\nu)t\right]/2 \\ \cos\omega t \cos 2\varphi \cos 2\nu t &= \cos 2\varphi \left[\cos(\omega + 2\nu)t + \cos(\omega - 2\nu)t\right]/2\,. \end{aligned} \tag{20}$$

Solution (19) after introduction (20) gives

$$\begin{aligned} u_a &= \frac{\sin 2\varphi \sin\left[(\omega + 2\nu)t - \psi_{a1}\right]}{2\sqrt{(\Omega_{20}^2 - (\omega + 2\nu)^2)^2 + \beta^2(\omega + 2\nu)^2}} - \frac{\sin 2\varphi \sin\left[(\omega - 2\nu)t - \psi_{a2}\right]}{2\sqrt{(\Omega_{20}^2 - (\omega - 2\nu)^2)^2 + \beta^2(\omega - 2\nu)^2}} \\ u_a &= \frac{\cos 2\varphi \cos\left[(\omega + 2\nu)t - \psi_{b1}\right]}{2\sqrt{(\Omega_{20}^2 - (\omega + 2\nu)^2)^2 + \beta^2(\omega + 2\nu)^2}} + \frac{\cos 2\varphi \cos\left[(\omega - 2\nu)t - \psi_{a2}\right]}{2\sqrt{(\Omega_{20}^2 - (\omega - 2\nu)^2)^2 + \beta^2(\omega - 2\nu)^2}}\,. \end{aligned} \tag{21}$$

The phase angles are

$$\psi_{a1} = \psi_{b1} = \tan^{-1} \frac{\beta(\omega + 2\nu)}{\Omega_{20}^2 - (\omega + 2\nu)^2}$$
$$\psi_{a2} = \psi_{b2} = \tan^{-1} \frac{\beta(\omega - 2\nu)}{\Omega_{20}^2 - (\omega - 2\nu)^2}. \qquad (22)$$

For graphical representation of these decomposition, the time history of equation (20) for $\varphi = 0$, $\omega = 6$ and $\nu = 2$ is shown in Fig. 9. The input force excitation with angular frequency $\omega = 6$ is drawn in the first row a). Its product with $\cos(2\nu t)$ corresponding to the running of excitation force on the disk with angular frequency $\nu = 2$ is recorded in second row b). Bottom two curves c), d) give harmonic components of the signal b).
Response of rotating disk on the excitation components contain the same harmonic components c), d) but their magnitudes are influenced by the dynamic amplification coefficients different for $(\omega + 2\nu)$ and $(\omega - 2\nu)$. These amplification coefficients depend for perfect disk on common eigenfrequency Ω_{20} (n = 2, l = 0) and on damping β.

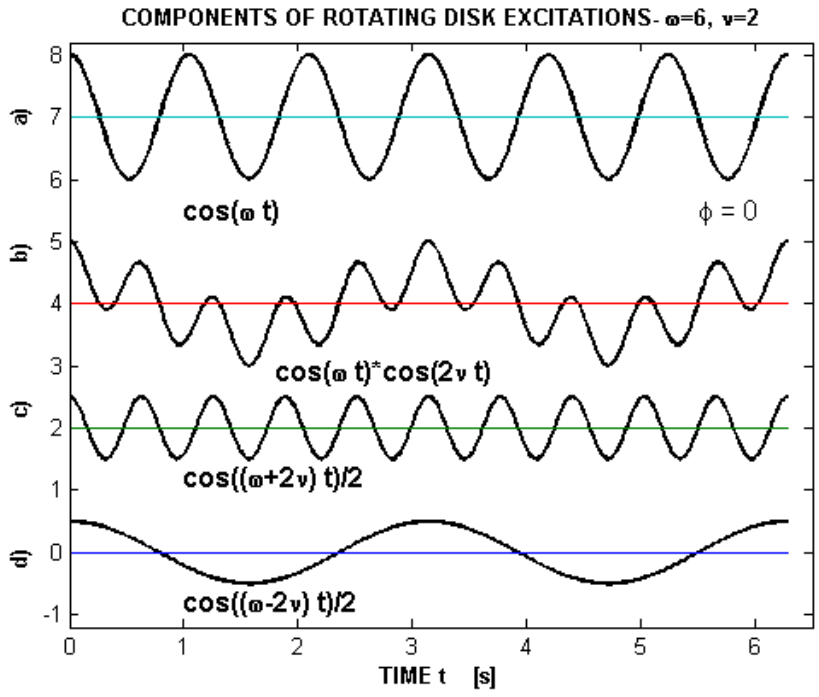

Fig. 9

There dynamic amplification coefficients are

$$\text{for } (\omega + 2\nu): \quad \Omega_{20}^2 \Big/ \sqrt{(\Omega_{20}^2 - (\omega + 2\nu)^2 + \beta^2 (\omega + 2\nu)^2}$$
$$\text{for } (\omega - 2\nu): \quad \Omega_{20}^2 \Big/ \sqrt{(\Omega_{20}^2 - (\omega - 2\nu)^2 + \beta^2 (\omega - 2\nu)^2} \qquad (23)$$

The entire response of rotating disk on space fixed harmonic excitation $F_0 \cos \omega t$ with increasing excitation frequency can be ascertained after connected both components (21) into one expression.

$$u(\varphi,t,\omega) = u_a + u_b =$$

$$= \frac{\cos(2\varphi - (\omega+2\nu) + \psi_1)}{2\sqrt{(\Omega_{20}^2 - (\omega+2\nu)^2 + \beta^2(\omega+2\nu)^2}} + \frac{\cos(2\varphi + (\omega-2\nu) - \psi_2)}{2\sqrt{(\Omega_{20}^2 - (\omega-2\nu)^2 + \beta^2(\omega-2\nu)^2}} \tag{24}$$

where $\psi_1 = \tan^{-1}\dfrac{\beta(\omega+2\nu)}{\Omega_{20}^2 - (\omega+2\nu)^2}$, $\psi_2 = \tan^{-1}\dfrac{\beta(\omega-2\nu)}{\Omega_{20}^2 - (\omega-2\nu)^2}$

Let us choose disk eigenfrequency $\Omega_{20} = 250$ and damping $\beta = 10$, speed of disk rotation let be $\nu = 20$. Time histories of both components u_a and u_b are shown in Fig. 10 for exciting frequency $\omega = 210$ and in Fig. 11 for frequency $\omega = 290$, all in one point the disk at $\varphi = 0$.

In the first case, the component u_a with frequency

$$\omega = \Omega_{20} - 2\nu = 250 - 2.20 = 210 s^{-1} \tag{25a}$$

comes into resonance (Fig. 10), in the second case the component u_b with frequency

$$\omega = \Omega_{20} + 2\nu = 250 + 2.20 = 290 s^{-1} \tag{25b}$$

is in resonance as seen in Fig. 11.

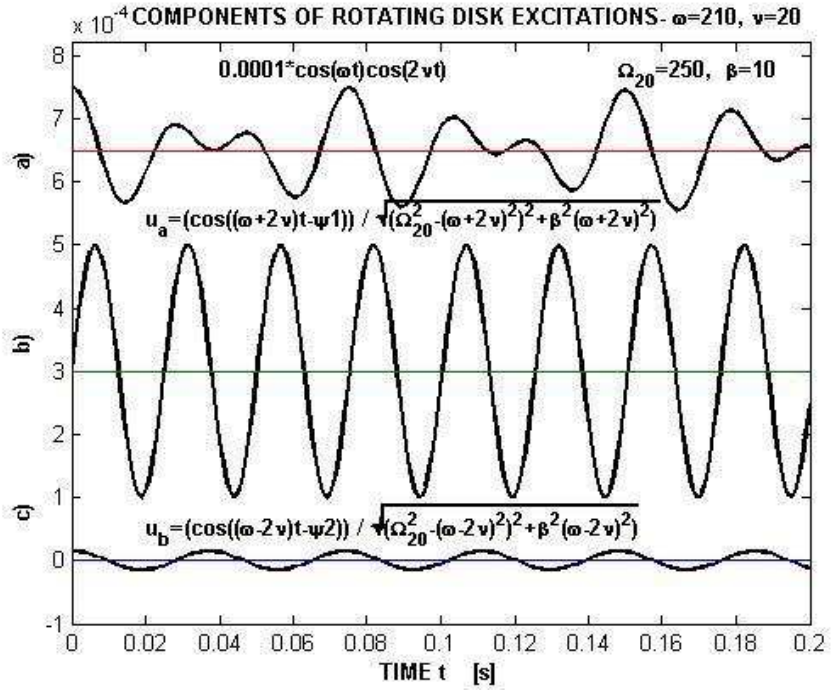

Fig. 10

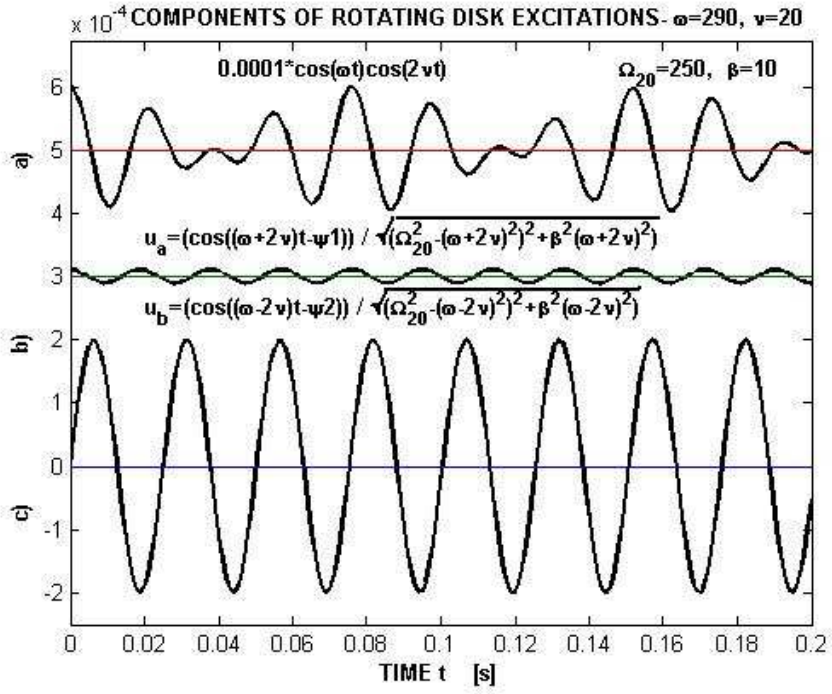

Fig. 11

The speed ν of disk rotation influences frequency position of resonance peaks. This effect is demonstrated in Fig. 12, where a set of response curves at constant $\Omega_{20} = 250$, $\beta = 10$ and at different disk speed $\nu = 0 - 15$ step 2.5 is drawn in excitation frequency range $\omega = \langle 200,300 \rangle s^{-1}$. Non-rotating disk has only one resonance at $\omega = 250 s^{-1}$. Disk rotation splits this resonance peak into two peaks, which shift to the lower and higher frequencies. It is caused by existence of two travelling waves in rotating disk excited in space fixed point.

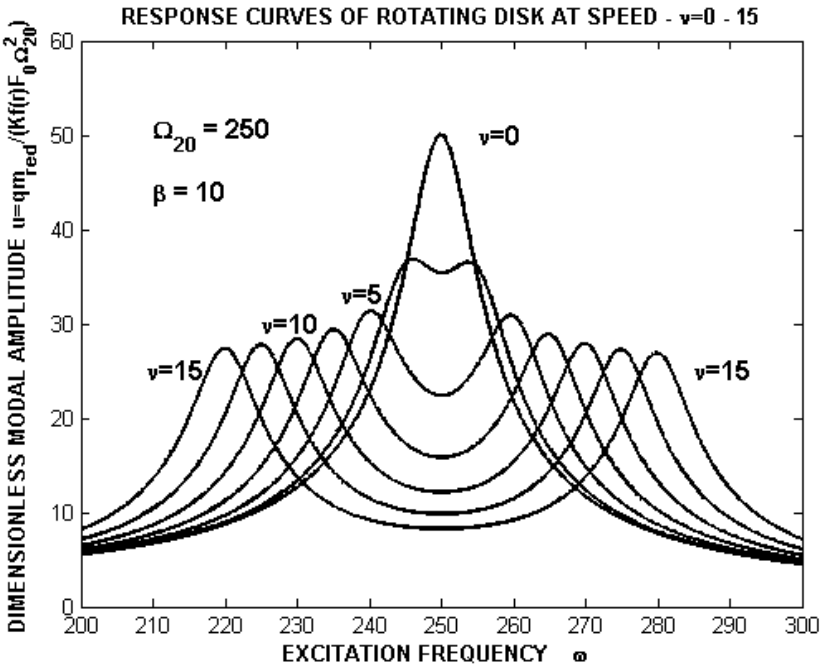

Fig. 12

4. Conclusion

It has been shown that in the circular disk fixed its centre exist double eigenfrequencies with two orthogonal modes of vibrations. Nodal diameters are arbitrary at perfect disks, but have fixed position at imperfect disks. Analysis of dynamic properties of non-rotating imperfect linearly damped disk excited by an external harmonic transversal force $F_0 \cos \omega t$ shows the existence of travelling waves, which intensity depends on the position of point of force application. Detail analysis was focused on the modes with two modal diameters. Response of stationary perfect disk on harmonic excitation is only stationary oscillation without any travelling waves.

Response of rotating disk both perfect or imperfect (speed *v*) harmonically excited in fixed point in space contains always travelling waves. Analysis focused on the frequency range near the resonance of mode with two nodal diameters proves the existence of two resonances split due to the travelling waves.

Presented study is a contribution to the theoretical support of experimental research of rotating model of bladed disk carried out in our Institute. The future extension of this theoretical analysis will include the investigation of nonlinear elastic and damping properties of rotating disk, as well as the influence of elastic, mass and damping imperfections on the dynamic behaviour of rotating disk.

5. Acknowledgement

This work has been elaborated in a frame of the grant project GA CR 101/09/1166 “Research of dynamic behaviour and optimalization of complex rotating system with non-linear couplings and high damping materials”.

6. References

1. Půst, L. (1985) Vlijanie nesověršenstv v symmetrii těl vraščenija na jich kolebanija, in: *Proc. V. National Congress on Theoretical and Aplied Mechanics* (G. Brankov, ed.), Pub. House Bulgarian AS, Sofia, Vol. 3, p. 131 – 136.
2. Půst, L. & Veselý, J. (1988) Kmitání nevyváženého lopatkového kola II. *Zpráva č. Z 1091/88,* Institute of Thermomechanics, Praque, 47 p.
3. Malík, M. (1988) Vynucené kmitání tlumeného kroužku, *Diplomová práce*, ČVUT-FJFI, Praha, 78 str.
4. Půst, L. (1986) Aplikovaná mechanika kontinua II. *Dynamika kontinua*, skripta, ČVUT-FJFI, Praha, 122 str.
5. Tobias, S.A. & Arnold, R.N. (1957) The Influence of Dynamical Imperfection on the Vibration of Rotating Disks, *Proc. Inst. Mech*. Engrs, 171, Edinburgh, p. 669-690.
6. Torii, T & Yasuda, K. (1999) Nonlinear Oscillation of a Rotating Disk Subject to a Transverse Load at a Space-fixed Point, in: *X. World Cong. on the Theory of Machine and Mechanisms* (T. Leinonen, ed.), Oulu, Finland, p. 1752-1757.
7. Qikan Li (1990) The Experimental Analysis for Lateral Vibration Characteristics of Disk-Shaped Bevel Gear , in: *3rd International Conf. on Rotordynamics* – IFToMM (Lalanne, M., ed.), Lyon, p. 553-556.

8. Bucher, I., et al. (2004) Real-time travelling waves and whirl decomposition, in: *Proc. 8th Int. Conf. on Vibrations in Rotating Machinery* (D.J.Ewins, ed), IMechE 2004, p. 261-267.

9. Yan Li-Tang & Li Qi-Han (1990) Investigation of Travelling Wave Vibration for Bladed Disk in Turbomachinery, in: *Proc. 3rd Int. Conf. on Rotordynamics*– IFToMM (Lalanne, M., ed.), Lyon, p.133-135.

10. Raman, A. & Mate, C.D.Jr. (1999) Slowly Modulated Travelling Waves in Circular Plates Spining Near Critical Speed, in: *Proc. of DETC´99*, ASME, Las Vegas, VIB-8050, p. 1-16.

11. Vaněk, F., et al. (2008) Buzení rezonančního kmitání lopatek oběžných kol magnetickým polem, in: *Proc. Parní turbiny a jiné turbostroje 2008*, (Šťastný M. ed), Plzeň, Škoda, p.19/1-19/10.

12. Pešek, L., et al. (2008) Dynamics of Rotating Blade Disk Identifical by Magneto-Kinematic Measuring System, in: *Proc. ISMA 2008*, (Sas, P., Bergen, B., eds), Katholieke Univ. Leuven, p. 1097-1111

13. Pešek, L., et al. (2009) Development of Excitation and measurement for identification of rotating blade disk, in: *Proc. SIRM 2009, Int. Conf. On Vibrations in Rotating Machines*, TU Vienna, ID-8, p. 1-10

14. Procházka, P., et al. (2009) Rozšíření a zpřesnění vibradiagnostického systému pro výzkum kmitání rotujících součástí strojů, in: *Proc. Dynamics of Machines 2009* (Pešek, L., ed.) IT ASCR, Praha, p. 97-105